Unbiased Detection of Cysteine Sulfenic Acid by 473 nm Photodissociation Mass Spectrometry: Toward Facile In Vivo Oxidative Status of Plasma Proteins

Jean-Valery Guillaubez, Delphine Pitrat, Yann Bretonnière, Jérôme Lemoine, Marion Girod

▶ **To cite this version:**

Jean-Valery Guillaubez, Delphine Pitrat, Yann Bretonnière, Jérôme Lemoine, Marion Girod. Unbiased Detection of Cysteine Sulfenic Acid by 473 nm Photodissociation Mass Spectrometry: Toward Facile In Vivo Oxidative Status of Plasma Proteins. Analytical Chemistry, 2021, 93 (5), pp.2907-2915. 10.1021/acs.analchem.0c04484 . hal-03151805

HAL Id: hal-03151805
https://hal.science/hal-03151805

Submitted on 25 Feb 2021

HAL is a multi-disciplinary open access archive for the deposit and dissemination of scientific research documents, whether they are published or not. The documents may come from teaching and research institutions in France or abroad, or from public or private research centers.

L'archive ouverte pluridisciplinaire **HAL**, est destinée au dépôt et à la diffusion de documents scientifiques de niveau recherche, publiés ou non, émanant des établissements d'enseignement et de recherche français ou étrangers, des laboratoires publics ou privés.

Unbiased detection of cysteine sulfenic acid by 473 nm photodissociation mass spectrometry: towards facile *in vivo* oxidative status of plasma proteins

Jean-Valery Guillaubez[1], Delphine Pitrat[2], Yann Bretonnière[2], Jérôme Lemoine[1], Marion Girod[1]

[1] Univ Lyon, CNRS, Université Claude Bernard Lyon 1, Institut des Sciences Analytiques, UMR 5280, 5 rue de la Doua, F-69100 VILLEURBANNE, France.

[2] Univ Lyon, ENS de Lyon, CNRS UMR 5182, Université Lyon I, Laboratoire de Chimie, F-69342 Lyon (France)

Corresponding author: Marion Girod, Email : marion.girod@univ-lyon1.fr

Abstract

Cysteine (Cys) is prone to diverse post-translational modifications in proteins, including oxidation into sulfenic acid (Cys-SOH) by reactive oxygen species generated under oxidative stress. Detection of low concentrated and metastable Cys-SOH within complex biological matrices is challenging due to the dynamic concentration range of proteins in the samples. Herein, visible laser-induced dissociation (LID) implemented in a mass spectrometer was used for streamlining the detection of Cys oxidized proteins thanks to proper derivatization of Cys-SOH with a chromophore tag functionalized with a cyclohexanedione group. Once grafted, peptides undergo a high fragmentation yield under LID, leading concomitantly to informative backbone ions and to a chromophore reporter ion. 79 % of the Cys-containing tryptic peptides deriving from human serum albumin and serotransferrin tracked by Parallel Reaction Monitoring (PRM) were detected as targets subjected to oxidation. These candidates, as well as Cys-containing peptides predicted by *in silico* trypsin digestion of 5 other human plasma proteins, were then tracked in real plasma samples to pinpoint the endogenous Cys-SOH subpopulation. Most of the targeted peptides were detected in all plasma samples by LID-PRM, with significant differences in their relative amounts. By eliminating the signal of interfering co-eluted compounds, LID-PRM surpasses conventional HCD-PRM in detecting grafted Cys-SOH containing peptides and allows now to foresee clinical applications in large human cohorts.

Keywords

chromophore derivatization, cysteine oxidation, laser induced dissociation, mass spectrometry

INTRODUCTION

The human body is regulated, amongst other processes, by a balance between oxidative and reductive conditions. With aging, under chronic exposition to environmental factors, or as very recently suggested as a consequence of the cytokine storm associated with SARS Cov-2 infection,[1] excess production of reactive oxygen species (ROS) can accumulate and disturb normal cell physiology and signaling pathways. Cysteine (Cys) is a principal target for ROS oxidation.[2] Cys sulfenic acid (SOH) is the first step on the path towards other redox modifications of the cysteine residue, such as disulfide formation or over-oxidation to irreversible sulfinic acid (SO_2H) and sulfonic acid (SO_3H). A diverse set of reducing enzymes can recycle oxidized Cys back to their reduced state.[3] This reversible oxidation process of cysteine residues into sulfenic acid has been identified as an on-and-off redox switch that regulates cellular signals[3,4] and can affect catalytic activity, bio-molecular interactions and stability of target proteins.[5]

Therefore, monitoring modification of the Cys redox state in the proteome has emerged as an important field of research, leading to the development of a wide range of redox proteomic strategy.[6–9] However, the intrinsic unstable nature of the SOH Cys intermediate precludes from easy capture and measurement. Thus, most studies for protein thiols oxidation analysis indirectly make use of thiol-tagging maleimide or iodoacetamide derivatives. These approaches are based on the premise that the sub-fraction of proteins bearing oxidized thiol groups can be estimated through the decrease of signal of the reduced-state population.[7,10] Another indirect method lies in first blocking the free Cys with an alkylating reagent, then reducing the sample (with arsenite, TCEP or DTT) to make the new thiols available for labelling with a specific tag.[8] Different probe can be used for thiol derivatization, such as biotinylated iodoacetamide, biotin-HPDP (Biotin switch) or fluorescent reagent,[6] allowing affinity- or

fluorescence- based detection after 2D electrophoresis (SDS-PAGE).[8,11] However, all these methods using spectroscopic, fluorescent or immune-enzymatic detection allow only a global qualitative detection of the amount of oxidized proteins but do not provide any information on the extent of oxidative damage and their localization for each specific protein present in complex cellular extracts or biofluids.

Hence, liquid chromatography (LC) coupled to tandem mass spectrometry-based (MS/MS) methodologies have been developed to accurately pinpoint cysteine oxidation sites. Isotope coded affinity tags (ICAT) were specifically designed for thiol trapping[10,12,13] containing a cleavable biotin tag and a linker which exists in isotopically light and heavy forms, to differentially labeled initially oxidized versus free Cys residues. Thiol-reacting iodoacetyl isobaric tandem mass tags (iodoTMT) have been also developed for the study of cysteine oxidation.[14–16] Different isobaric TMTs have been conceived with the concept that the collisional activation process yields reporter ions to streamline both the detection of Cys-containing peptides and their quantification through the comparison of reporter ion intensities. However, these techniques do not directly target the sulfenic acid but, indirectly, the reduced SH form. Few studies reported the direct trapping of cysteine sulfenic acid by nucleophiles[17] such as norbornene[18] or –dione derivative probes.[19–24] MS analysis of cysteine sulfenic acid modification in intact proteins after derivatization with cyclohexanedione probes has been reported.[20,21] Depending on the molecular mass variation, the number and amount of sulfenic acid cysteine residues can be assigned. Bottom-up strategies in data dependent acquisition (DDA) allows to analyze individual sites, enabling site-specific identification and relative quantification,[25] while absolute quantification has been even performed by the use of an isotope coded tag.[21] Due to the dynamic range of protein concentration in whole trypsin

hydrolysates, these methods require a pre-fractionation or enrichment step of the sub-population of oxidized proteins[25].

The added value of the exquisite fragmentation specificity provided by laser-induced dissociation to detect a peptide sub-population has been highlighted many times, for instance with infrared multiphoton photodissociation (IRMPD) at 10.6 μm for targeting sulfonated peptides.[26,27] Intrinsic chromophores such as disulfide bonds or tyrosine residues have been similarly used for specific detection in the ultraviolet range (UVPD).[28,29] The grafting of amino-acid side chains with proper chromophore is an alternative for introducing specificity at the fragmentation step. With the aim of targeting Cys-containing peptide, this concept has been implemented using the judicious selection of chromophores absorbing in the UV range at 351 nm[30] and 266 nm[31,32] or in the visible range at 473 nm.[33–35]

In the present work, we unveil a strategy coupling mass spectrometry and LID at 473 nm for streamlining the detection of cysteine sulfenic acid-containing peptides in complex protein digests. A new Dabcyl chromophore probe functionalized with a cyclohexanedione group was designed in order to ensure controlled grafting of SOH moieties, hence conferring specific absorption property at 473 nm of oxidized peptides. Having optimized the tagging conditions from *in vitro* oxidized model peptides and proteins, a multiplexed targeted LID-Parallel Reaction Monitoring (PRM) strategy was deployed to monitor *in vivo* oxidized Cys-SOH peptides of human plasma proteins after trypsin digestion, without enrichment step. As anticipated, the fragmentation specificity provided by LID results in the dramatic improvement of the signal attributed to cysteine-SOH containing peptides in complex tryptic digests.

EXPERIMENTAL SECTION

Details about chemicals, chromophore synthesis and NMR characterization, instrumental set-up and HPLC conditions are provided in Supporting Information (SI).

Standard Protocol Approvals, Registrations and Patient Consents

All subjects gave written informed consent for participation in this study. For those with substantial cognitive impairment, a caregiver, legal guardian, or other proxy gave consent. The study protocols were reviewed and approved by the appropriate Institutional review boards (CCPRB Brest, n°970-436-001 and CCPRB Lille, n°92/68).

Synthesis of the Dabcyl cyclohexanedione chromophore

Probe **1** (DabDn) was obtained in excellent yield by esterification with 4-[2-[4-(dimethylamino)phenyl]diazenyl]-benzoic acid (Dapcyl) of the free alcohol function of known 3-ethoxy-6-(3-hydroxypropyl)cyclohex-2-enone **2**, followed by acidic hydrolysis to liberate the 1,3-cyclohexadione moiety (Scheme S1).[22]

Sample preparation

For the oxidation and derivatization of the model peptides, 100 µL of LCTVATLR (LR8) or LGADMEDVGR peptides at 100 µM in water and 100 µL of probe **1** DabDn at 100 µM in dimethyl sulfoxide (DMSO) were mixed together, then 100 µL of oxygen peroxide (H_2O_2) at 100 µM were added to obtain a 1-1-1 peptide-DabDn-H_2O_2 molar ratio. After various reaction times (between 1 and 24 h), 10 µL were pipetted and diluted into 90 µL of water/acetonitrile (H_2O/ACN) 70/30 +0.1 % formic acid (F.A). The same conditions were applied for the oxi-derivatization of 10 synthetic peptides pooled at a theoretical individual concentration of 200 µg/mL in H_2O/ACN (50/50) + 0.5 % of FA.

In order to estimate the limit of quantification, the oxi-derivatized LR8 peptide was diluted in a complex digest of serum. For this, 10 µL of human serum were mixed with 40 µL urea 8 M and 5.5 µL dithiothreitol (DTT) at 150 mM in ammonium bicarbonate (AMBIC) 50 mM, then denaturated at 60°C for 40 min. Samples were cooled at room temperature and 17 µL of iodoacetamide (IAM) 150 mM in AMBIC 50 mM were added. Samples were put in the dark at RT for 40 min, then diluted with 3 mL of 50 mM AMBIC. Digestion was performed with 10 µL of a 2 mg/mL trypsin solution at 37°C overnight. After digestion, samples were desalted and concentrated by SPE (Oasis HLB 3cc) and eluted with 1.5 mL methanol (MeOH).[33] Eluted samples were dried at 40°C under N_2 stream and resuspended into 200 µL of a H_2O/ACN 70/30 +0.1 % F.A solution, according to the spiked LR8 volume. LR8 sample, after 8 h of oxidation/derivatization reaction, was diluted into a 33/66 DMSO/H_2O solution and spiked into plasma samples. 9 samples of concentrations 2, 5, 20, 60, 100, 120, 160, 180 and 200 nM of oxi-derivatized LR8 were prepared alongside with a non-spiked "blank" plasma sample. Each sample was made in triplicate.

For the oxidation and derivatization of the protein mixture, 250 µL of Human Serum Albumin (HSA) and Human Transferrin (TransfH) at 1 mg/mL each were mixed in order to obtain a total of 500 µg of proteins. 5.4 µL DTT at 150 mM in AMBIC (3 fold molar excess) were added and proteins were denaturated and reduced at 60°C during 40 min. Samples were cooled at room temperature, then 500 µL of 538 µM DabDn in DMSO were added, followed by 500 µL of 538 µM H_2O_2 after mixing, and left to react during 6-8 h at room temperature. Digestion of oxi-derivatized proteins was performed with 10 µL of a 2 mg/mL trypsin solution at 37°C overnight. Samples were purified by SPE on Oasis HLB 3cc cartridge, eluted with 1.5 mL MeOH, dried at 40°C under N_2 stream and resuspended in 200 µL of a H_2O/ACN 70/30 +0.1 % F.A solution.

For the derivatization of endogenous oxidized cysteine in plasma samples, 10 µL of human plasma were mixed with 40 µL urea 8 M, then denaturated at 60°C for 40 min. Samples were cooled at room temperature, diluted with 194.5 µL of H_2O, then 250 µL of 1.637 mM DabDn in DMSO were added, followed by 250 µL of H_2O after mixing, to reach a 33% organic/aqueous phase ratio. Samples were left to react during 7 h at room temperature. Digestion of oxi-derivatized proteins was performed with 10 µL of a 2 mg/mL trypsin solution at 37°C overnight. Samples were purified by SPE as previously mentioned and resuspended in 200 µL of a H_2O/ACN 70/30 +0.1 % F.A solution.

Instrumentation and mass spectrometry operating conditions

Experiments were performed on a modified hybrid quadrupole-orbitrap QExactive® mass spectrometer (Thermo Fisher Scientific, San Jose, CA, USA) equipped with a HESI ion source. Electrospray ionization in HESI source was achieved on positive mode with a spray voltage of 4 kV at 320°C, and sheath gas and auxiliary gas flow rates were 12 and 4 (arbitrary unit), respectively. The AGC target was set to 1e6, pairing with a maximum injection time at 100 ms, and the S-Lens RF level set to 55 (arb. unit). Resolution @ *m/z* 200 in the orbitrap analyzer was set to 140,000 for DabDn characterization and 35,000 for PRM analysis. For MS/MS analysis, isolation of the precursor was defined with a ± 2.0 *m/z* window in order to select full isotopic patterns. PRM list of precursors is available in the Supporting Information (Table S1 for the 2 proteins and Table S2 for the plasma samples). For LID fragmentation, the activation time was set to 25 ms with an activation energy of only 3 eV in order to inject ions within the HCD cell but avoid CID contaminating events.[33] For higher-energy collisional dissociation (HCD), activation time was set to 3 ms with an activation energy ranging from 19 to 24 eV depending on the precursor ion.

RESULTS AND DISCUSSION

Characterization of the new chromophore DabDn.

Several dimedone-based derivatives have recently been synthesized to label –SOH proteins, including biotinylated dimedone analogues[7,22] for affinity purification or fluorophore-linked dimedone analogues[22] for visualization. Herein, our strategy was to add a chromophore group to the dimedone probe in order to induce absorption properties in the visible range. The Dabcyl chromophore is a non-fluorescent quencher used as acceptor in Förster resonance energy transfer (FRET) applications. Moreover, we previously showed that Dabcyl maleimide has a high photo-dissociation yield between 450 and 540 nm and is well suited for LID analysis.[35] Thus, a new probe combining a reacting cyclohexanedione group and a Dabcyl chromophore has been designed for specific derivatization of -SOH moieties (probe **1**) and for conferring to the end-product absorption property at 473 nm. The structure of the probe **1** DabDn chromophore can be found in Scheme 1. The protonated adduct of the DabDn is detected at *m/z* 422.2083 ($C_{24}H_{28}O_4N_3$, mass error: -1.5203 ppm) in positive mode ESI-MS (Figure S1). Protonated dimer $[2DabDn+H]^+$ is also detected at *m/z* 843.4052. The LID spectrum at 473 nm of the protonated DabDn is shown in Figure 1a. Laser irradiation yields to the depletion of the precursor ion signal and the production of several fragment ions. The most intense ion at *m/z* 252.112 is a characteristic reporter ion of the Dabcyl chromophore, arising from the fragmentation between the carbonyl carbon and the ester oxygen. This reporter ion can be used to pinpoint derivatized oxidized peptides from reconstructed ion chromatogram. The DabDn chromophore has a high photo-fragmentation ratio of 99.3 % after 3 ms of irradiation time. This intense fragmentation yield is also observed between 460 and

550 nm, as shown by the optical spectrum of the protonated chromophore recorded on a linear ion trap coupled with an OPO laser[36] (Figure S2).

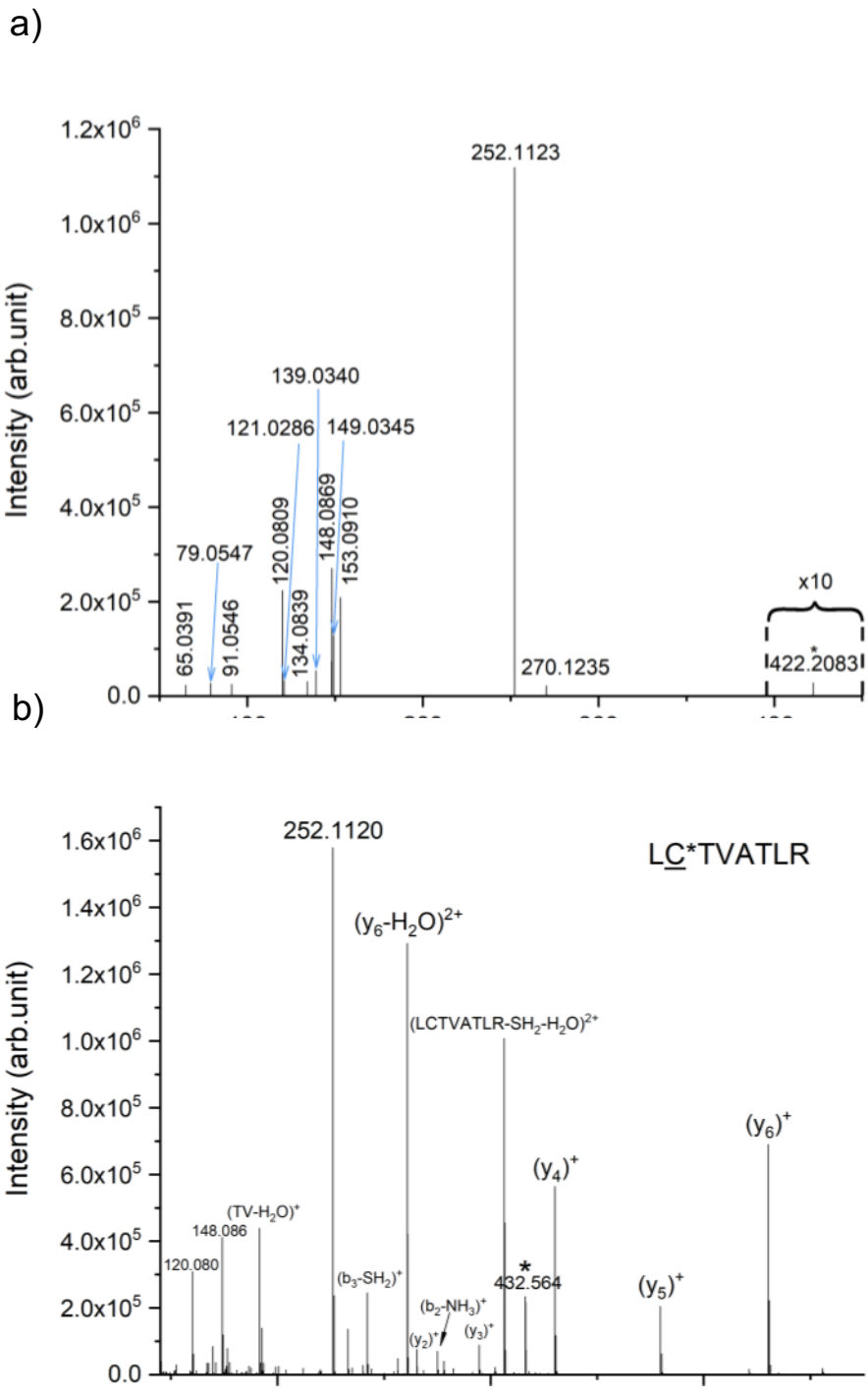

Figure 1. LID spectrum of a) the protonated DabDn chromophore at *m/z* 422.208 with 3 ms of irradiation time and b) the triply protonated oxi-derivatized peptide LC*TVATLR at *m/z* 432.564 with 25 ms of irradiation time and laser power 450 mW. The asterisk shows the

precursor ions. All ion assignments are supported by accurate mass measurements (errors <6 ppm). The photo-dissociation yields were 99.3 % and 97 % for the Dabcyl chromophore and the oxi-derivatized LC*TVATLR peptide, respectively.

Peptide *in vivo* oxidation and chromophore derivatization.

Effectiveness of SOH derivatization with DabDn chromophore was assessed with the model LCTVATLR peptide containing one cysteine. At first, oxidation of cysteine was performed using hydrogen peroxide H_2O_2, a strong oxidant involved in oxidative stress, since no Cys-SOH peptide standard are available. Unfortunately, SOH group is sensitive to electrospray ionization (ESI) process,[9] which precludes the direct observation of cysteine-oxidized peptides. Furthermore, H_2O_2 excess leads to irreversible over-oxidation of SOH into SO_2H and SO_3H, as well as dimer formation. To help monitor the oxidation rate, we then carried out concomitantly cysteine oxidation and derivatization of SOH groups with the cyclohexanedione chromophore (reaction is shown in Scheme 1). The electrospray mass spectrum of the solution post reaction reveals a predominant triply protonated oxi-derivatized peptide $[LC^*TVATLR]^{3+}$, as well as a less intense doubly protonated form. The LID spectrum of the triply charged species at *m/z* 432.564 (Figure 1b) exhibits informative singly charged b and y peptide backbone fragment ions, allowing the peptide sequencing, as well as the intense reporter ion (*m/z* 252.112) arising from internal fragmentation within the chromophore (see Scheme 1). The LID fragmentation of the oxi-derivatized peptide also leads to the formation of two LID-specific fragments of DabDn at *m/z* 120.080 and *m/z* 148.086. The observation of fragmentation of the peptide backbone is a clear evidence that part of the energy, initially localized at the chromophore, must be redistributed across the entire system. Fragmentation between the chromophore linker and the cysteine side chain (see Scheme 1) is also observed

from the precursor ion (annotated LCTVATLR-SH_2-H_2O in Figure 1b) indicating the importance of the linker in the energy redistribution. b_3 fragment ion is also observed after elimination of the chromophore and the thiol group (annotated b_3-SH_2 in Figure 1b). After 25 ms of irradiation, the photodissociation yield of the triply charged oxi-derivatized peptide is about 97 %, a value only slightly lower compared to the DabDn chromophore alone (99 % see Figure 1a). The high fragmentation yield reached after a short irradiation time shows the compatibility of the approach with chromatographic separation.

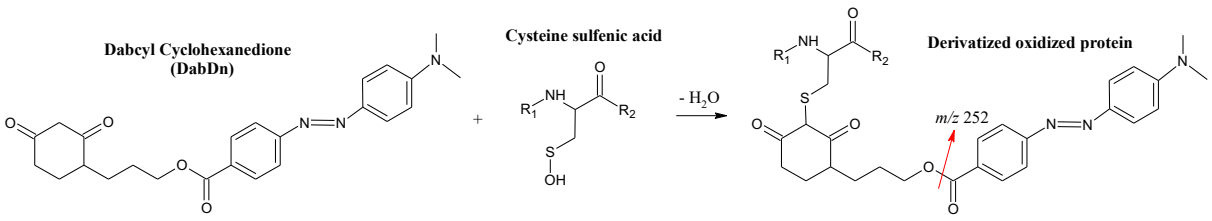

Scheme 1. Derivatization reaction of cysteine sulfenic acid with chromophore DabDn.

As depicted in the reconstructed chromatogram Figure 2, LC*TVATLR oxi-derivatized peptide, $[M(SDabDn)]^{3+}$, is the main species formed in the presence of H_2O_2 and DabDn. Furthermore, two forms of oxi-derivatized peptides, $[M(SDabDn)+O]^{3+}$, were detected with an additional oxygen. In both cases, the cysteine was oxidized and derivatized, and over-oxidation was located on the initial L (at RT=14.7 min) and on one of the last three T/L/R (at RT=15.15 min) (low *m/z* fragment ions are lacking but would be required to accurately locate the additional oxygen). Due to the DabDn high hydrophobicity, oxi-derivatized peptides are eluted at a higher retention time than the native forms. This behavior should favor their detection in highly complex tryptic digest by extracting them from the predominant bulk of non-derivatized peptides. The oxi-derivatization reaction is not total since non-oxidized, hence non-derivatized peptide $[M(SH)]^{2+}$ remains (Figure 2). As a control of LID specificity, this non-

oxidized (NO) form at *m/z* 438.752 is not photo-fragmented (Figure S3). The Cys of the initial peptide was also irreversibly over-oxidized in sulfinic $[M(SO_2H)]^{2+}$ and sulfonic $[M(SO_3H)]^{2+}$ acids, due to the use of H_2O_2 as oxidizing reagent. Peptide dimers $[M(SS)M]^{4+}$ are also observed after oxidation of Cys in the form of disulfide bond. Eventually, some low intense mono and dioxidized peptides on other amino acids than cysteine were detected. A chromatographic representation of the different forms of mono-oxidation is shown in Figure S4.

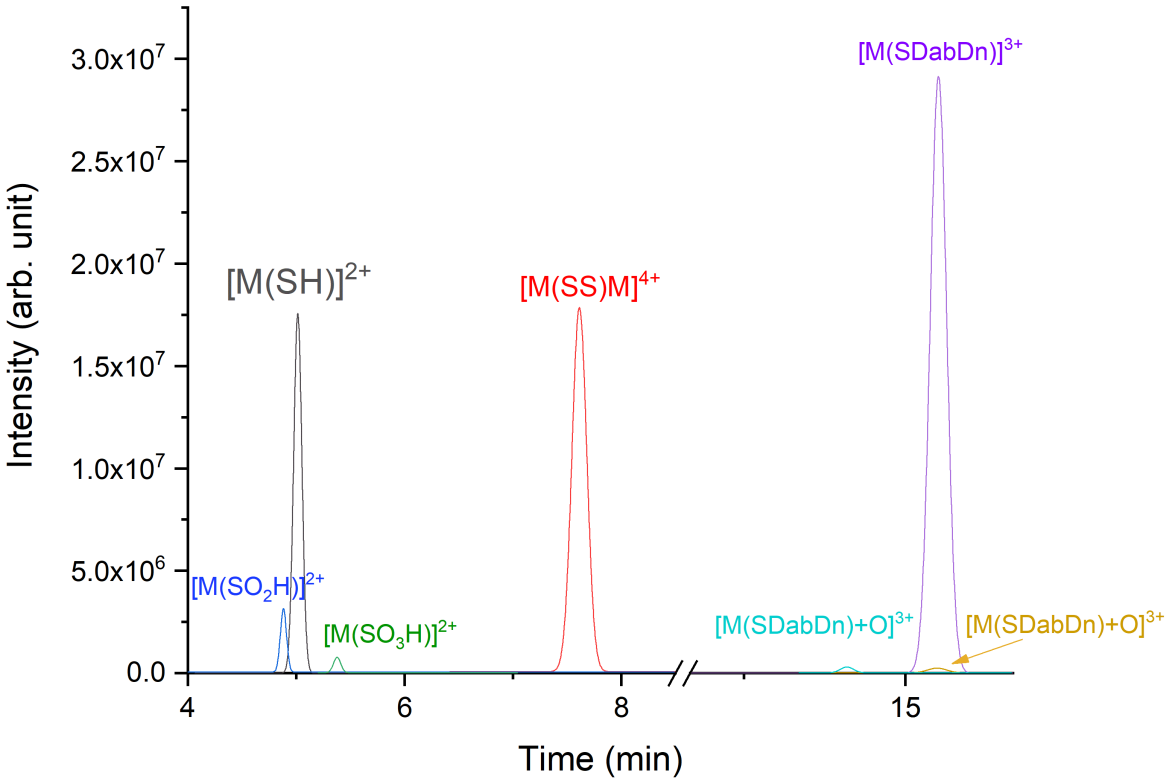

Figure 2. Reconstructed chromatogram of the separation of the different forms produced after 9 h of oxi-derivation of the LCTVATLR model peptide in presence of H_2O_2 and DabDn, analyzed in full MS.

The effectiveness of one-pot oxidation of Cys-thiol group into SOH and subsequent derivatization with DabDn chromophore has been successively demonstrated. However, it is essential to ensure the specificity of SOH reactivity toward the coupling reagent in order to avoid any false positive reaction. Methionine is a sulfur-containing amino acid that is prone to oxidation leading to methionine sulfoxide ($R_2S=O$). Therefore, the presence of oxidized methionine could eventually give rise to artefactual derivatization that needs to be assessed. Oxi-derivatization tests were conducted on a single methionine-containing model peptide LGADMEDVR submitted to the same reaction with H_2O_2 and DabDn. The methionine oxidized form was detected (structure confirmed by HCD fragmentation in Figure S5), while neither chromophore adduct nor reporter ion signal were detectable (no signal on XICs from the LID analysis in Figure S6). This confirms the strict specificity of DabDn towards SOH group.

During the optimization of the reaction, several key-parameters affecting the formation of the cysteine oxi-derivatized peptide were highlighted. H_2O_2 yields the formation of SOH but also induces over-oxidation and dimer formation. The peptide-H_2O_2 molar ratio was thus optimized to favor the production of the oxi-derivatized peptide LC*TVATLR. Moreover, as the chromophore is not soluble in water, large amounts of organic solvent (such as DMSO or MeOH) are required in order to ensure proper derivatization while avoiding chromophore precipitation. Thus, the type of solvent and its percentage in the reaction phase have been optimized to promote the formation of the oxi-derivatized peptide and corresponding product areas are presented in Figure 3 along with the reaction time. Other parameters such as the temperature or pH did not lead to significant improvement of the reaction yield, and therefore will not be presented here. The formation of cysteine oxi-derivatized peptide increases with time. Moreover, the highest amount of cysteine oxi-derivatized peptide was formed using DMSO as organic solvent (black lines in Figure 3). This could be explained by the higher

solubility of DabDn in DMSO or by the possible formation of H bonds with thiol group in MeOH,[37] which could preserve the cysteine from oxidation. Furthermore, for both MeOH and DMSO solvents, the lowest percentage of organic phase tested (33%, squares) induces a greater formation of oxi-derivatized peptide. Both 1-1 and 10-1 peptide-H_2O_2 molar ratio used with DMSO lead to an equivalent amount of cysteine oxi-derivatized peptide until 7 h ofreaction where a plateau is reached with a 1-10 ratio (dashed line in Figure 3). The oxi-derivatization keep going for a 1-1 ratio (plain line). However, more over-oxidation and dimer formation are observed with a 1-10 peptide-H_2O_2 ratio (data not shown). Therefore, in order to minimize these side-reactions, a 1-1 peptide-H_2O_2 ratio is optimal.

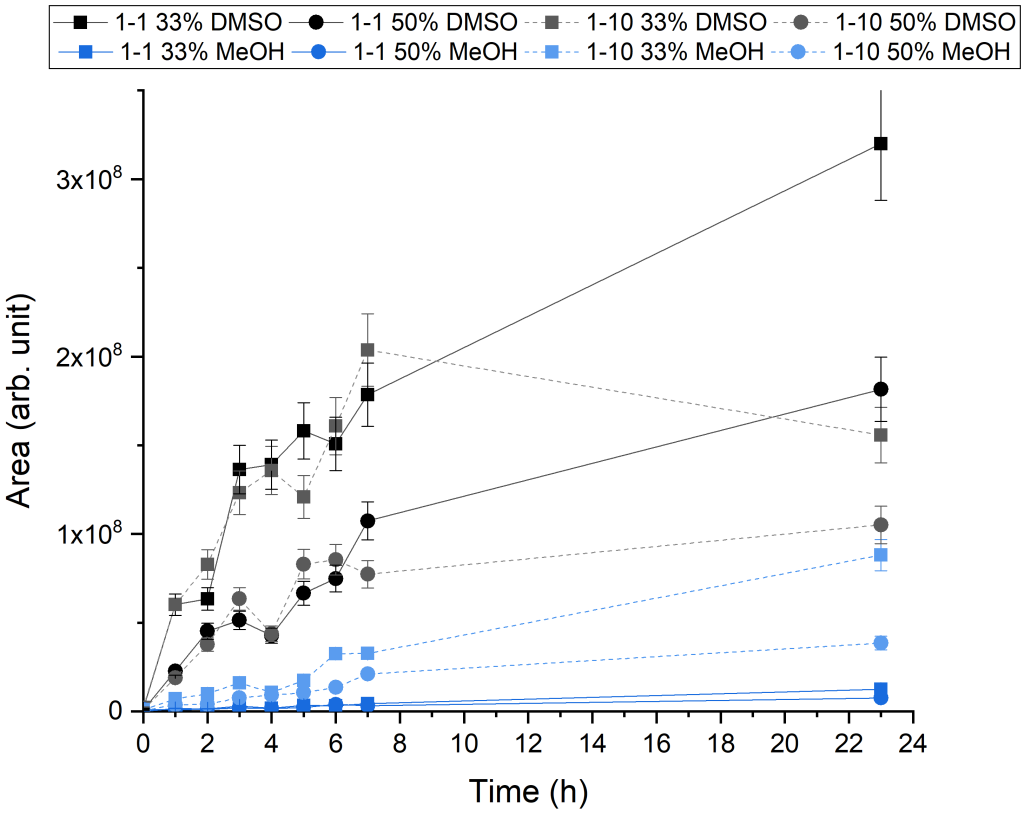

Figure 3. Kinetic of the formation of the oxi-derivatized model peptide LC*TVATLR with different % of organic phase: 33 % (squares) and 50 % (dots) of DMSO (black) or MeOH (blue);

and peptide-H_2O_2 ratio: 1-1 (plain line) and 1-10 (dashed line). Error bars represent the standard deviation on the area measurement (n=4) for each condition.

Thus, we established the optimal conditions of oxi-derivatization at a 1-1-1 peptide-H_2O_2-DabDn molar ratio in 33 % DMSO for 7 h. A 1-1 molar ratio between the DabDn and the non-oxidized peptide was used. Since the oxidation reaction is not total, DabDn will be in excess for the derivatization reaction of the cysteine-SOH form. This is confirmed by the absence of significant increase of oxi-derivatized peptide formation upon addition of chromophore. These conditions of oxi-derivatization were applied on 10-pooled synthetic Cys-containing peptides, which were afterwards analyzed by PRM-LID. For each peptide, the derivatized Cys-SOH peptide was detected as illustrated by the reconstructed chromatograms in Figure S7a. All Cys-SOH were derivatized with the DabDn and specifically fragmented in LID, yielding the reporter ion and backbone fragment ions (Figure S7b). The different synthetic peptides presented the same ability for oxi-derivatization, showing the broad applicability of the method for detection of oxidized Cys.

Unfortunately, since it is impossible to monitor and quantify the Cys-SOH oxidized peptide, the derivatization yield is not directly accessible. However, an oxidation/derivatization percentage yield can be calculated by dividing the amount of product by the theoretical molar yield, i.e. the molar amount of the initial NO peptide. The molar amount of oxi-derivatized LR8 peptide cannot be directly calculated from the MS signal because no standard is available and ionization efficiency is unknown. However, the amount of formed product can be estimated by the amount of DabDn reactant consumed. As illustrated by Figure S8, the signal decrease of the DabDn is associated with the oxi-derivatized LR8 peptide formation. Therefore, the oxi-derivatized molar amount corresponds to the molar amount of consumed DabDn

(development of equations can be found in SI). Since the molar ratio between the non-oxidized LR8 peptide and the DabDn chromophore is 1-1, the molar yield is finally calculated by dividing the amount of consumed DabDn (area at T_0 - area at T) by the area of the initial DabDn peak at the beginning of the reaction (T_0). The oxi-derivatization percentage yield varies from 20 to 40 % between different analyses, as the oxidation reaction is not fully controlled.

Linearity and limit of quantification (LOQ) of oxi-derivatized the LCTVATLR peptide in a complex matrix

In order to assess the linearity, the sensitivity and the precision of the detection by LID, the oxi-derivatized LR8 peptide was spiked into digested human serum to obtain a final concentration ranging from 2 nM to 200 nM (no signal was detected below 2 nM). Dilution ratios were based on the 20 % oxi-derivatization yield calculated for the initial oxi-derivatized peptide concentration. For the quantification carried out in parallel reaction monitoring mode (PRM), the area of 5 transitions corresponding to the 3 main peptide fragments ($[y6\text{-}H_2O]^{2+}$, $[y6]^+$ and $[y4]^+$) and the 2 LID-specific fragments (*m/z* 252.112 and 148.086 see Figure 1b) were summed.

By analyzing the results of experiments performed in triplicate, coefficient of determination values of the response curves measured by LID-PRM demonstrated a linearity over 2 orders of magnitude with all R^2 better than 0.99 (Figure S9). Imprecision values of peak areas expressed by the coefficient of variation (CV) were lower than 20 % for all concentrations (Table 1). All back-calculated standard concentrations were within ±15 % deviation from the nominal value, corresponding to accuracy in the acceptable range of 85-115 % (Table 1). LOQ

was estimated to 2 nM, which corresponds to the lowest concentration of the linearity range with a CV lower than 20 %.

Regarding the HCD-PRM experiments, no oxi-derivatized LR8 signal was detected at the lowest 2 nM concentration level (insert in Figure S9), while a CV of 74 % was obtained at 5 nM (Table 1), which is out of the validation range. Therefore, the LOQ achieved in HCD-PRM mode is between 5 and 20 nM. Moreover, poor accuracy is observed in HCD from the concentration of 60 nM and below. Altogether, these results unambiguously highlight the marked improvement of sensitivity and accuracy performances provided by the exquisite specificity of LID.

Table 1. Precision and accuracy data of back-calculated concentrations of calibration samples for replicated oxi-derivatized LR8 peptide spiked at different concentration into human serum in LID and HCD mode. N/A indicates that the peptide was not detected at this concentration. Underlined values are out of the range for the analytical method validation, i.e. CV < 20 % and accuracy ranging 85–115 %.

Nominal Concentration (nM)	**LID**			**HCD**		
	Mean back-calculated concentration (nM)	Accuracy (%)	CV (%)	Mean back-calculated concentration (nM)	Accuracy (%)	CV (%)
2	2.3	115	20	0	<u>N/A</u>	<u>N/A</u>
5	4.4	88	17	1.7	<u>34</u>	<u>74</u>
20	18.6	93	9	27.6	<u>138</u>	9
60	51.6	86	16	75.6	<u>126</u>	9
100	102	102	13	93	93	5
120	126	105	16	130.8	109	6
160	163.2	102	8	147.2	92	11
180	183.6	102	12	178.2	99	15
200	194	97	18	204	102	5

Oxi-derivatization of Cysteine-containing model proteins

The applicability of the method for the detection of oxidized cysteine in a complex proteome was mimicked with a mixture of 2 abundant proteins of the human plasma (Human Serum Albumin – HSA, and Human Serotransferrin – TransfH). Proteins were first denaturated and reduced with DTT to make more cysteine residues available for oxidation and derivatization. The 1-1-1 peptide-H_2O_2-DabDn ratio was adapted to a 1-1-1 cysteine-H_2O_2-DabDn ratio from the total amount of cysteine of the 2 proteins and the reaction was performed with 33 % of DMSO, following the optimal conditions deduced from the experiments with the LR8 model peptide. Proteins were digested *in silico* and 33 peptides containing one single cysteine were selected as potential targets of oxi-derivatization for subsequent targeted analysis in PRM mode. Chromatographic separation and retention time windows were optimized (Table S1). Remarkably, due to the high proton affinity of the DabDn, charge states observed for derivatized peptides are often higher than for their native form. Overall, 26 cysteine oxi-derivatized peptides were successfully detected (reconstructed chromatograms are presented in Figure S10). The LID method allows to detect 78.8 % of the targeted Cys sites after oxidation and derivatization of the 2 proteins (Table S1).

Finally, the specificity of LID compared to the non-discriminating HCD mode was also highlighted by the extracted PRM ion chromatograms of the reporter ion at *m/z* 252.1 from a control experiment where the 2 protein mixture was not subjected to oxidation prior to PRM analysis (Figure S11). For this control sample, which does not contain oxi-derivatized peptides, no signal is detected in LID, unlike in HCD mode where ion signals at *m/z* 252.1 arising from interfering fragmentation pathways are detected at distinct retention times. Hence, the LID analysis results in the decrease of the background noise.

Detection of endogenous cysteine oxidation in plasma samples

Having optimized the grafting of Cys-OH containing peptides by the DabDn chromophore and assessed the analytical performances of their detection by LID-PRM, the method was ultimately implemented to pinpoint endogenous cysteine sulfenic acid-containing peptides in human plasma. The relevance of such quantification is illustrated by studies reporting on the central contribution of HSA cysteine trioxidation in redox processes in plasma[38–40] and especially as a potential biomarker for diabetes disease[41] since HSA is the most abundant thiol in plasma.

Thus, a multiplexed LID-PRM assay was designed *in silico* to track in 6 human plasma samples the putative Cys-OH form of the 26 peptide candidates detected above for HSA and TransfH as well as for 91 additional cysteine containing peptides deriving from 5 other concentrated human proteins. Plasma samples were denatured and directly allowed to react with the DabDn chromophore in order to derivatize and block the endogenous Cys-OH groups, with a 1-1 Cys-DabDn ratio (calculated according to the concentration of thiols in human plasma[40]) and 33 % of DMSO, and then reduced and digested with trypsin. Following the analysis of the 6 plasma samples, 46 peptides with derivatized endogenous oxidized cysteine were successfully identified (Table S3) among the 117 putative candidates (see Table S2), i.e. 39.3 % of the Cys sites. Backbone fragmentation observed in LID allowed to confirm the sequence of the derivatized peptide and locate the individual site of oxidation. For HSA protein, among all cysteine-containing peptides pinpointed after *in vitro* oxidation of the commercial protein, only the one containing C487 was not detected. In the case of TransfH, among the 17 oxidized peptides previously detected in the model study, only those containing the C19 and C345 residues were not detected. This could be due to a reduced reactivity of these two residues towards endogenous oxidative stress compared to the *in vitro* oxidative condition for which

the protein was likely partially unfolded after the disulfide bridge reduction. As an attempt to correlate the oxidation propensity with the secondary structure, Cys-OH sites were highlighted on the 3D structure of those 2 proteins (Figure S12). Interestingly, for the TransfH, 11 Cys-OH sites over 15 were located in beta-strand features (yellow in Figure S12b), while the C19, C355, C402, C418 and C523, which are not detected as –SOH, belong to the alpha-helix region of the protein (red in Figure S12b). Moreover, amino acids present in the core of the protein could be less accessible for the solvent interaction than those at the surface. For the HSA, the oxidized Cys are located mainly in alpha-helix features (Figure S12a) and the non-oxidized C200, C289 and C487 are in the hydrophobic core of the protein, while C316 is located at the surface. Therefore, the secondary structure alone is not sufficient to account for the susceptibility of Cys residues to oxidize. Indeed, many structural parameters influence the Cys-OH susceptibility, such as sequential distance to the nearby cysteine, solvent accessibility, pKa or secondary structure.[42–44] Finally, 3 to 6 peptides containing a derivatized Cys-OH were detected for the other proteins, indicating that these Cys sites are more sensitive to endogenous oxidation. Therefore, this method could be used to provide a valuable insight into the relationship of protein structure and susceptibility to oxidation.

Examples of chromatographic overlay of transitions observed for derivatized Cys-oxidized peptides, as well as the corresponding sequence, are presented Figure S13. The high signal to noise ratios allows confident relative quantification of oxidized peptides between the 6 plasma samples (all values can be found in Table S3). Figure 4 shows the relative amount of oxidized proteins between the 6 plasma samples analyzed by LID-PRM. Differences in global protein oxidation levels can be observed between the different plasma samples, #2 sample being the more oxidized one, while protein oxidation levels were lower for samples #4 and #6. Considering individual proteins, we can notice that the relative amounts of Cys-oxidized CO3,

FIBB and FINC exhibit the most variation between the 6 plasma samples, while the Cys oxidation level of HSA and TransfH is more stable.

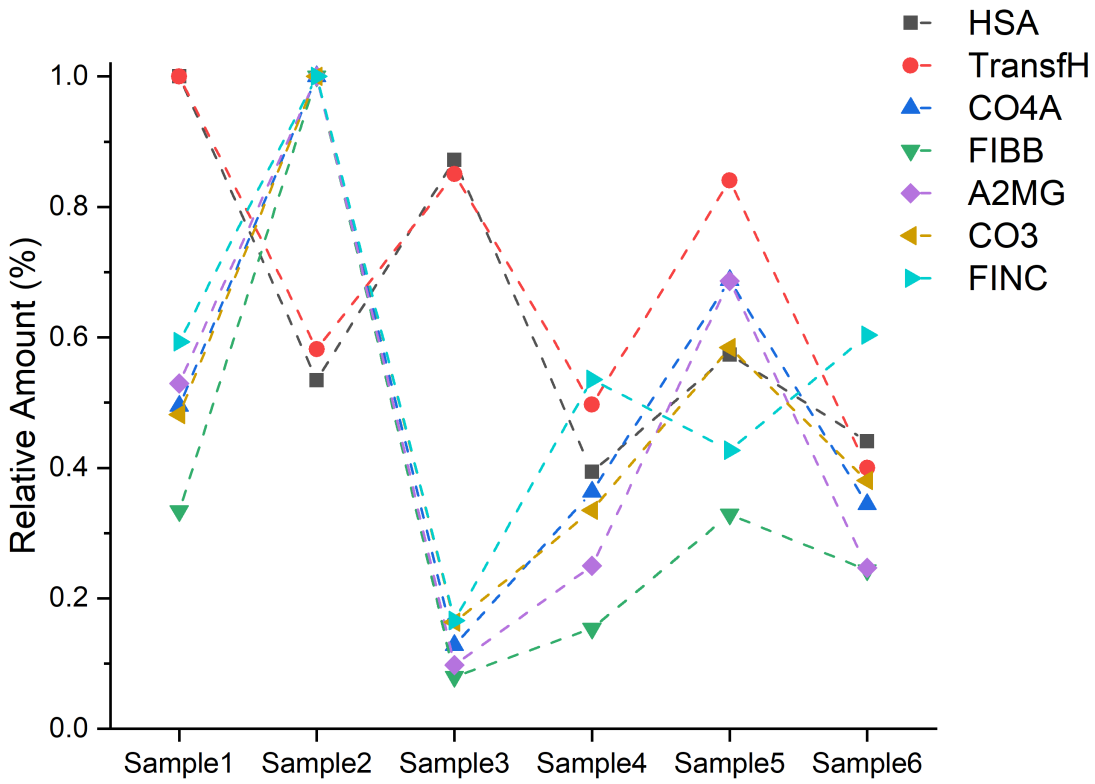

Figure 4. Relative quantification of oxidized proteins between the 6 plasma samples analyzed by LID-PRM. The relative amount of oxidized protein was calculated with the mean signal value of each individual derivatized endogenous oxidized Cys-containing peptides of a same protein. Normalization was made for each protein by dividing its mean signal intensity by the maximal signal intensity between the 6 samples.

In contrast to LID, only 39 derivatized Cys-OH containing peptides were detected in HCD for the same samples. The same oxidized peptides were detected for HSA from the 6 plasma samples in both LID and HCD. Figure 5 represents the comparative analysis of the plasma samples in LID and HCD for the 6 other proteins. 1 Cys-SOH containing peptide was not

detected (indicated by the red boxes) for CO4A and FINC proteins, 2 for the A2MG and 3 for the TransfH protein, in HCD compare to LID. For CO3 and FIBB proteins, oxidized Cys-peptides were detected in only 5 over 6 plasma samples (individual results can be found in Table S4). Indeed, lowest concentrated Cys oxidized peptides (i.e. smaller quantitative ratios in LID) could not been extracted.

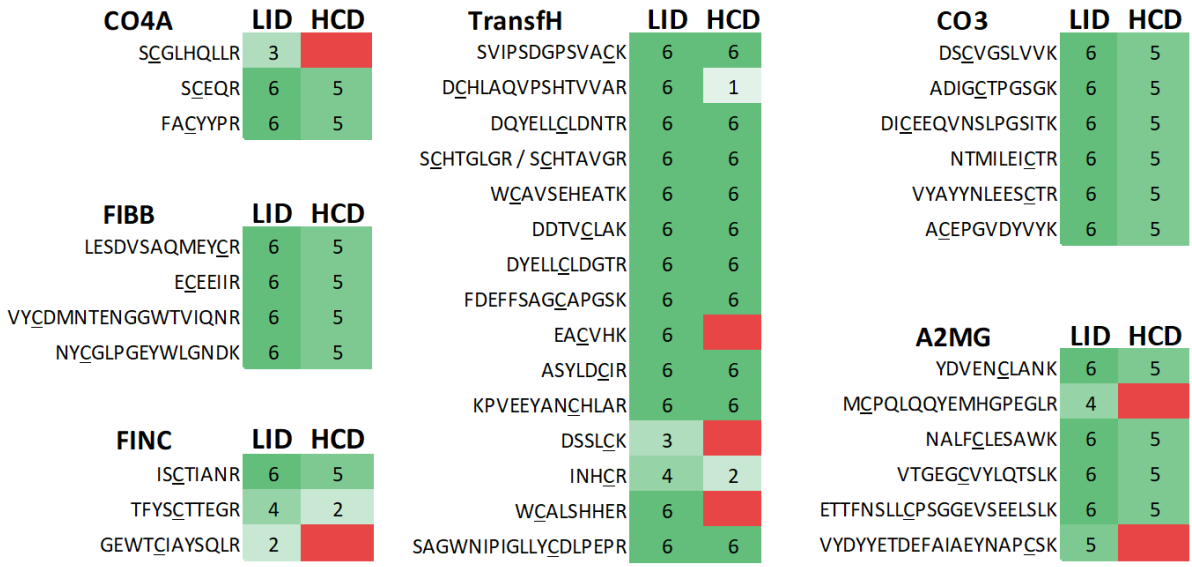

Figure 5. Comparison of the detection coverage obtained either by LID or HCD PRM experiments of derivatized endogenous oxidized Cys-containing peptide target across the 6 plasma samples, as a function of the protein identity. The number in the box and the green color intensity represents the number of plasma samples for which the oxidized peptide form was detected. The red boxes indicate that the peptide was not detected in any sample.

These results strengthen the concept that specific photo-fragmentation at 473 nm represents an effective strategy for *de novo* building of targeted PRM assays for unbiased detection and quantification of Cys sulfenic acid-containing peptides in large medical cohorts.

Conclusions

In this work, the specific detection of peptides harboring cysteine sulfenic acid was carried out by high-resolution mass spectrometry coupled to LID at 473 nm to add a stringent optical specificity to the mass selectivity. This new methodological approach relies on the controlled derivatization of Cys-SOH with an original Dabcyl chromophore functionalized by a cyclohexanedione group (DabDn). The experimental grafting conditions of Cys-SOH residues with the DabDn chromophore were optimized *in vitro* with H_2O_2 oxidized model peptides. No parasite tagging reaction towards oxidized methionine was observed, which is of prime importance considering the high reactivity of this residue in naturally occurring oxidative condition. Once grafted, oxi-derivatized Cys-peptides are easily and specifically pinpointed during on-line 473 nm LID analysis by reconstructing an ion chromatogram on a characteristic reporter ion. The LID fragmentation spectra of oxi-derivatized Cys-peptides also exhibit intense y and b fragment ions arising from backbone fragmentation, which are essential for peptide identification in discovery shotgun proteomics or in order to confirm a sequence in hypothesis-driven targeted experiments.

As a decisive illustration, endogenous Cys-SOH peptides deriving from 7 human plasma proteins were effectively targeted and directly detected in plasma samples by LID after chromophore derivatization, without any enrichment step. Compared to HCD, more oxidized peptides (46) were detected as a result of the LID specificity. Together, these results pave the way for streamlined and multiplexed targeted detection and quantification of endogenous low-concentrated oxidized cysteine residues. The typical fields of applications are the large-scale evaluation of the oxidative stress associated with human pathologies such as aging or neurodegenerative diseases. In a near future, the method will be applied for relative

quantification of Cys oxidized protein in a SARS Cov2 human cohort to test the hypothesis of the cytokine storm inducing massive release of ROS.

Acknowledgments

The research leading to these results received funding from the French Agence National de la Recherche under the Grant Agreement ANR-18-CE29-0002-01 HyLOxi.

Supporting Information

Details about chemicals, chromophore synthesis and NMR characterization, instrumental set-up and HPLC conditions. Details on calculation of the oxi/derivatization percentage yield. LID spectrum of the non-oxidized model peptide LCTVATLR. Chromatogram of the mono-oxidized peptide LCTVATLR. HCD spectrum of the methionine-oxidized model peptide LGADMEDVR, XIC of the methionine-oxidized, oxi-derivatized cysteine and reporter ion at *m/z* 252.11. Reconstructed chromatograms of 10 oxi-derivatized cysteine-containing synthetic peptides by LID-PRM and LID spectra. Kinetics of the DabDn consumption vs LCTVATLR oxidized cysteine derivatization. Calibration curves of the oxi-derivatized peptide spiked in plasma samples by HCD vs LID. LID-PRM analysis of the *in vitro* oxidized and derivatized mixture of HSA and TransfH. Comparison of the interference at *m/z* 252.1 in blank plasma sample between HCD and LID. 3D representation of endogenous oxidized cysteine in HSA and TransfH proteins. Examples of XIC chromatograms of 5 fragment ions detected for derivatized endogenous Cys-oxidized peptide in plasma sample by LID-PRM. PRM precursors lists used for oxi-derivatization and endogenous cysteine oxidation screening. Relative abundance of all detected endogenous oxidized cysteine between 6 plasma samples in HCD and LID analysis.

References

(1) Massaad, C.; Nuss, P.; Benoliel, J.-J.; Becker, C. Tissue Damage from Neutrophil-Induced Oxidative Stress in COVID-19. *Nat. Rev. Immunol.* **2020**, 1–2. https://doi.org/10.1038/s41577-020-0407-1.

(2) Paulsen, C. E.; Carroll, K. S. Cysteine-Mediated Redox Signaling: Chemistry, Biology, and Tools for Discovery. *Chem. Rev.* **2013**, *113* (7), 4633–4679. https://doi.org/10.1021/cr300163e.

(3) Poole, L. B.; Karplus, P. A.; Claiborne, A. Protein Sulfenic Acids in Redox Signaling. *Annu. Rev. Pharmacol. Toxicol.* **2004**, *44* (1), 325–347. https://doi.org/10.1146/annurev.pharmtox.44.101802.121735.

(4) Ilbert, M.; Horst, J.; Ahrens, S.; Winter, J.; Graf, P. C. F.; Lilie, H.; Jakob, U. The Redox-Switch Domain of Hsp33 Functions as Dual Stress Sensor. *Nat. Struct. Mol. Biol.* **2007**, *14* (6), 556–563. https://doi.org/10.1038/nsmb1244.

(5) Van Der Reest, J.; Lilla, S.; Zheng, L.; Zanivan, S.; Gottlieb, E. Proteome-Wide Analysis of Cysteine Oxidation Reveals Metabolic Sensitivity to Redox Stress. *Nat. Commun.* **2018**, *9* (1). https://doi.org/10.1038/s41467-018-04003-3.

(6) Devarie-Baez, N. O.; Lopez, E. I. S.; Furdui, C. M. Biological Chemistry and Functionality of Protein Sulfenic Acids and Related Thiol Modifications. *Free Radic. Res.* **2016**, *50* (2), 172–194. https://doi.org/10.3109/10715762.2015.1090571.

(7) Leonard, S. E.; Carroll, K. S. Chemical "omics" Approaches for Understanding Protein Cysteine Oxidation in Biology. *Curr. Opin. Chem. Biol.* **2011**, *15* (1), 88–102. https://doi.org/10.1016/j.cbpa.2010.11.012.

(8) Eaton, P. Protein Thiol Oxidation in Health and Disease: Techniques for Measuring Disulfides and Related Modifications in Complex Protein Mixtures. *Free Radic. Biol. Med.* **2006**, *40* (11), 1889–1899. https://doi.org/10.1016/j.freeradbiomed.2005.12.037.

(9) Furdui, C. M.; Poole, L. B. Chemical Approaches to Detect and Analyze Protein Sulfenic Acids. *Mass Spectrom. Rev.* **2014**, *33*, 126–146.

(10) Chiappetta, G.; Ndiaye, S.; Igbaria, A.; Kumar, C.; Vinh, J.; Toledano, M. B. *Proteome Screens for Cys Residues Oxidation: The Redoxome.*, 1st ed.; Elsevier Inc., 2010; Vol. 473. https://doi.org/10.1016/s0076-6879(10)73010-x.

(11) Yang, J.; Carroll, K. S.; Liebler, D. C. The Expanding Landscape of the Thiol Redox Proteome. *Mol. Cell. Proteomics* **2016**, *15* (1), 1–11. https://doi.org/10.1074/mcp.O115.056051.

(12) Ratnayake, S.; Dias, I. H. K.; Lattman, E.; Griffiths, H. R. Stabilising Cysteinyl Thiol Oxidation and Nitrosation for Proteomic Analysis. *J. Proteomics* **2013**, *92* (0), 160–170. https://doi.org/10.1016/j.jprot.2013.06.019.

(13) Leichert, L. I.; Gehrke, F.; Gudiseva, H. V.; Blackwell, T.; Ilbert, M.; Walker, A. K.; Strahler, J. R.; Andrews, P. C.; Jakob, U. Quantifying Changes in the Thiol Redox Proteome upon Oxidative Stress in Vivo. *Proc. Natl. Acad. Sci. U. S. A.* **2008**, *105* (24), 8197–8202. https://doi.org/10.1073/pnas.0707723105.

(14) Pan, K. T.; Chen, Y. Y.; Pu, T. H.; Chao, Y. S.; Yang, C. Y.; Bomgarden, R. D.; Rogers, J. C.; Meng, T. C.; Khoo, K. H. Mass Spectrometry-Based Quantitative Proteomics for Dissecting Multiplexed Redox Cysteine Modifications in Nitric Oxide-Protected Cardiomyocyte under Hypoxia. *Antioxidants Redox Signal.* **2014**, *20* (9), 1365–1381. https://doi.org/10.1089/ars.2013.5326.

(15) Shakir, S.; Vinh, J.; Chiappetta, G. Quantitative Analysis of the Cysteine Redoxome by Iodoacetyl Tandem Mass Tags. *Anal. Bioanal. Chem.* **2017**, *409* (15), 3821–3830. https://doi.org/10.1007/s00216-017-0326-6.

(16) Wojdyla, K.; Williamson, J.; Roepstorff, P.; Rogowska-Wrzesinska, A. The SNO/SOH

TMT Strategy for Combinatorial Analysis of Reversible Cysteine Oxidations. *J. Proteomics* **2015**, *113*, 415–434. https://doi.org/10.1016/j.jprot.2014.10.015.
(17) Gupta, V.; Paritala, H.; Carroll, K. S. Reactivity, Selectivity, and Stability in Sulfenic Acid Detection: A Comparative Study of Nucleophilic and Electrophilic Probes. *Bioconjug. Chem.* **2016**, *27* (5), 1411–1418. https://doi.org/10.1021/acs.bioconjchem.6b00181.
(18) Alcock, L. J.; Oliveira, B. L.; Deery, M. J.; Pukala, T. L.; Perkins, M. V.; Bernardes, G. J. L.; Chalker, J. M. Norbornene Probes for the Detection of Cysteine Sulfenic Acid in Cells. *ACS Chem. Biol.* **2019**, *14* (4), 594–598. https://doi.org/10.1021/acschembio.8b01104.
(19) Qian, J.; Klomsiri, C.; Wright, M. W.; King, S. B.; Tsang, A. W.; Poole, L. B.; Furdui, C. M. Simple Synthesis of 1,3-Cyclopentanedione Derived Probes for Labeling Sulfenic Acid Proteins. *Chem. Commun.* **2011**, *47* (32), 9203–9205. https://doi.org/10.1039/c1cc12127h.
(20) Rehder, D. S.; Borges, C. R. Possibilities and Pitfalls in Quantifying the Extent of Cysteine Sulfenic Acid Modification of Specific Proteins within Complex Biofluids. *BMC Biochem.* **2010**, *11* (1). https://doi.org/10.1186/1471-2091-11-25.
(21) Seo, Y. H.; Carroll, K. S. Quantification of Protein Sulfenic Acid Modifications Using Isotope-Coded Dimedone and Iododimedone. *Angew. Chemie - Int. Ed.* **2011**, *50* (6), 1342–1345. https://doi.org/10.1002/anie.201007175.
(22) Poole, L. B.; Zeng, B. B.; Knaggs, S. A.; Yakubu, M.; King, S. B. Synthesis of Chemical Probes to Map Sulfenic Acid Modifications on Proteins. *Bioconjug. Chem.* **2005**, *16* (6), 1624–1628. https://doi.org/10.1021/bc050257s.
(23) Freeman, F.; Adesina, I. T.; La, J. Le; Lee, J. Y.; Poplawski, A. A. Conformers of Cysteine and Cysteine Sulfenic Acid and Mechanisms of the Reaction of Cysteine Sulfenic Acid with 5,5-Dimethyl-1,3-Cyclohexanedione (Dimedone). *J. Phys. Chem. B* **2013**, *117* (50), 16000–16012. https://doi.org/10.1021/jp409022m.
(24) Klomsiri, C.; Nelson, K. J.; Bechtold, E.; Soito, L.; Johnson, L. C.; Lowther, W. T.; Ryu, S. E.; King, S. B.; Furdui, C. M.; Poole, L. B. *Use of Dimedone-Based Chemical Probes for Sulfenic Acid Detection Evaluation of Conditions Affecting Probe Incorporation into Redox-Sensitive Proteins.*, 1st ed.; Elsevier Inc., 2010; Vol. 473. https://doi.org/10.1016/S0076-6879(10)73003-2.
(25) Yang, J.; Gupta, V.; Carroll, K. S.; Liebler, D. C. Site-Specific Mapping and Quantification of Protein S-Sulphenylation in Cells. *Nat. Commun.* **2014**, *5* (May), 2–13. https://doi.org/10.1038/ncomms5776.
(26) Borotto, N. B.; McClory, P. J.; Martin, B. R.; Hakansson, K. Targeted Annotation of S-Sulfonylated Peptides by Selective Infrared Multiphoton Dissociation Mass Spectrometry. *Anal. Chem.* **2017**, *89* (16), 8304–8310. https://doi.org/10.1021/acs.analchem.7b01461.
(27) Wilson, J. J.; Brodbelt, J. S. Infrared Multiphoton Dissociation for Enhanced de Novo Sequence Interpretation of N-Terminal Sulfonated Peptides in a Quadrupole Ion Trap. *Anal. Chem.* **2006**, *78* (19), 6855–6862. https://doi.org/10.1021/ac060760d.
(28) Joly, L.; Antoine, R.; Broyer, M.; Dugourd, P.; Lemoine, J. Specific UV Photodissociation of Tyrosyl-Containing Peptides in Multistage Mass Spectrometry. *J. Mass Spectrom.* **2007**, *42* (6), 818–824. https://doi.org/10.1002/jms.
(29) Agarwal, A.; Diedrich, J. K.; Julian, R. R. Direct Elucidation of Disulfide Bond Partners Using Ultraviolet Photodissociation Mass Spectrometry. *Anal. Chem.* **2011**, *83* (17), 6455–6458. https://doi.org/10.1021/ac201650v.
(30) Cotham, V. C.; Wine, Y.; Brodbelt, J. S. Selective 351 Nm Photodissociation of Cysteine-Containing Peptides for Discrimination of Antigen-Binding Regions of IgG

Fragments in Bottom-Up Liquid Chromatography-Tandem Mass Spectrometry Workflows. *Anal. Chem.* **2013**, *85* (11), 5577–5585. https://doi.org/10.1021/ac400851x.
(31) Diedrich, J. K.; Julian, R. R. Site Selective Fragmentation of Peptides and Proteins at Quinone Modified Cysteine Residues Investigated by ESI-MS. *Anal Chem.* **2011**, *82* (10), 4006–4014. https://doi.org/10.1021/ac902786q.Site.
(32) Parker, W. R.; Holden, D. D.; Cotham, V. C.; Xu, H.; Brodbelt, J. S. Cysteine-Selective Peptide Identification: Selenium-Based Chromophore for Selective S-Se Bond Cleavage with 266 Nm Ultraviolet Photodissociation. *Anal. Chem.* **2016**, *88* (14), 7222–7229. https://doi.org/10.1021/acs.analchem.6b01465.
(33) Girod, M.; Biarc, J.; Enjalbert, Q.; Salvador, A.; Antoine, R.; Dugourd, P.; Lemoine, J. Implementing Visible 473 Nm Photodissociation in a Q-Exactive Mass Spectrometer: Towards Specific Detection of Cysteine-Containing Peptides. *Analyst* **2014**, *139* (21), 5523–5530. https://doi.org/10.1039/C4AN00956H.
(34) Garcia, L.; Lemoine, J.; Dugourd, P.; Girod, M. Fragmentation Patterns of Chromophore-Tagged Peptides in Visible Laser Induced Dissociation. *Rapid Commun. Mass Spectrom.* **2017**, *31* (23), 1985–1992. https://doi.org/10.1002/rcm.7984.
(35) Enjalbert, Q.; Girod, M.; Simon, R.; Jeudy, J.; Chirot, F.; Salvador, A.; Antoine, R.; Dugourd, P.; Lemoine, J. Improved Detection Specificity for Plasma Proteins by Targeting Cysteine-Containing Peptides with Photo-SRM. *Anal. Bioanal. Chem.* **2013**, *405* (7), 2321–2331. https://doi.org/10.1007/s00216-012-6603-5.
(36) Antoine, R.; Dugourd, P. Visible and Ultraviolet Spectroscopy of Gas Phase Protein Ions. *Phys. Chem. Chem. Phys.* **2011**, *13* (37), 16494. https://doi.org/10.1039/c1cp21531k.
(37) Lobo, I. A.; Robertson, P. A.; Villani, L.; Wilson, D. J. D.; Robertson, E. G. Thiols as Hydrogen Bond Acceptors and Donors: Spectroscopy of 2-Phenylethanethiol Complexes. *J. Phys. Chem. A* **2018**, *122* (36), 7171–7180. https://doi.org/10.1021/acs.jpca.8b06649.
(38) Nagumo, K.; Tanaka, M.; Chuang, V. T. G.; Setoyama, H.; Watanabe, H.; Yamada, N.; Kubota, K.; Tanaka, M.; Matsushita, K.; Yoshida, A.; Jinnouchi, H.; Anraku, M.; Kadowaki, D.; Ishima, Y.; Sasaki, Y.; Otagiri, M.; Maruyama, T. Cys34-Cysteinylated Human Serum Albumin Is a Sensitive Plasma Marker in Oxidative Stress-Related Chronic Diseases. *PLoS One* **2014**, *9* (1). https://doi.org/10.1371/journal.pone.0085216.
(39) Li, H.; Grigoryan, H.; Funk, W. E.; Lu, S. S.; Rose, S.; Williams, E. R.; Rappaport, S. M. Profiling Cys34 Adducts of Human Serum Albumin by Fixed-Step Selected Reaction Monitoring. *Mol. Cell. Proteomics* **2011**, *10* (3), 1–13. https://doi.org/10.1074/mcp.M110.004606.
(40) Turell, L.; Radi, R.; Alvarez, B. The Thiol Pool in Human Plasma: The Central Contribution of Albumin to Redox Processes. *Free Radic. Biol. Med.* **2013**, *65*, 244–253. https://doi.org/10.1016/j.freeradbiomed.2013.05.050.
(41) Paramasivan, S.; Adav, S. S.; Ngan, S. F. C.; Dalan, R.; Leow, M. K. S.; Ho, H. H.; Sze, S. K. Serum Albumin Cysteine Trioxidation Is a Potential Oxidative Stress Biomarker of Type 2 Diabetes Mellitus. *Sci. Rep.* **2020**, *10* (1), 1–12. https://doi.org/10.1038/s41598-020-62341-z.
(42) Mapes, N. J.; Rodriguez, C.; Chowriappa, P.; Dua, S. Residue Adjacency Matrix Based Feature Engineering for Predicting Cysteine Reactivity in Proteins. *Comput. Struct. Biotechnol. J.* **2019**, *17*, 90–100. https://doi.org/10.1016/j.csbj.2018.12.005.
(43) Sanchez, R.; Riddle, M.; Woo, J.; Momand, J. Prediction of Reversibly Oxidized Protein Cysteine Thiols Using Protein Structure Properties. *Protein Sci.* **2008**, *17* (3),

473–481. https://doi.org/10.1110/ps.073252408.
(44) Sun, M. an; Zhang, Q.; Wang, Y.; Ge, W.; Guo, D. Prediction of Redox-Sensitive Cysteines Using Sequential Distance and Other Sequence-Based Features. *BMC Bioinformatics* **2016**, *17* (1), 1–10. https://doi.org/10.1186/s12859-016-1185-4.

Table of Contents